Bol. Soc. Paran. Mat.
©SPM – E-ISSN-2175-1188
SPM: www.spm.uem.br/bspm

(3s.) **v. 2025 (43) 2** : 1–22.
ISSN-0037-8712
doi:10.5269/bspm.78878

Finite Element Methods via Cubic Hermite Shape Functions for a Singularly Perturbed Boundary Value Problem with Mixed Shifts

Vivek K. and R. Nageshwar Rao*

ABSTRACT: In this paper, Galerkin finite element method is developed for a singularly perturbed differential equation with mixed shifts. Fitted operator and fitted mesh approaches are utilized for discretization. Cubic Hermite shape functions are chosen as basis functions in developing the method. Comparison of maximum absolute errors for the solutions of test problems is done for the proposed methods. Graphs are plotted to demonstrate the effect of shifts on the solution of the problem.

Key Words: Singular perturbation problems, differential-difference equations, numerical methods, finite element method, basis functions.

Contents

1. Introduction

A singular perturbation problem (SPP) is a problem that depends on a small positive parameter commonly known as the perturbation parameter (ϵ) and the solution to this problem behaves non-uniformly as $\epsilon \to 0$. Furthermore, a class of differential-difference equations is characterized by the presence of negative or positive shift terms and the highest-order derivative multiplied by ϵ. These types of problems model various physiological phenomena, such as fluid dynamics, heat transfer, as well as in specific structural mechanics problems that are modeled on thin domains. The solution of a singularly perturbed differential-difference equation (SPDDE) typically includes boundary layers along the boundary of the domain. These layers make the numerical study more difficult and hence need to be carefully taylored to adapt to the layer behaviour of the solution.

Singular perturbation problems have been extensively studied and several numerical methods have been proposed for the last few decades [1,2]. SPDDEs arise from mathematical models that hold practical significance, particularly in the fields of biology and physics [3,4]. Prathap and Rao [5] constructed numerical methods that employ non-polynomial splines, particularly emphasizing spline in compression, tension, and adaptive spline to tackle singularly perturbed boundary value problems with mixed shifts

* Corresponding author.
2010 *Mathematics Subject Classification:* 65L10, 65L11, 65L20, 65L50, 65L60, 65L70.
Submitted September 09, 2025. Published December 19, 2025

using fitted mesh. Ravi Kanth and Murali [6] proposed a numerical technique that utilizes the exponentially fitted spline method to solve singularly perturbed convection delay problems. Ranjan and Prasad [7] presented a new uniform mesh based exponentially fitted finite difference scheme, for a singularly perturbed differential-difference equation with delay and advance parameters. Vivek and Rao [8] developed exponentially fitted numerical schemes based on spline in compression and adaptive spline methods to solve a singularly perturbed differential-difference equation with mixed shifts. Kadalbajoo and Sharma [9] devised an ϵ-uniform numerical scheme based on a fitted mesh approach for solving SPDDEs with small shifts. Kadalbajoo et al. [10] discussed numerical solution of the problems arising from singularly perturbed general differential-difference equation by fitted operator finite difference method and fitted mesh finite difference method. Sirisha et al. [11] proposed a mixed finite difference method for solving a singularly perturbed differential-difference equation with mixed shifts. Conor [12] extended the Petrov-Galerkin upwind finite element method to variable coefficient problems in one dimension. In [13], the authors Singh et al. developed a numerical algorithm using trigonometric B-spline functions to approximate the solution of singularly perturbed boundary value problems. Singh and Kumar [14] constructed a numerical scheme comprising the quadratic B-splines on an exponentially graded mesh for the fourth-order singularly perturbed boundary value problem of an ordinary differential equation. Singh et al. [15] proposed a numerical method for solving fourth-order singularly perturbed linear and nonlinear boundary value problems of convection-diffusion type. Ayalew et al. [16] introduced an exponentially fitted fourth-order numerical approach for solving SPDDEs and investigated the effects of delay and advance parameters on the solution profile. Kumar [17] employed B-spline collocation approach to approximate the solution of SPDDEs with mixed shifts. Farshid and Seyede [18] worked out a computational method for approximate solution of singularly perturbed differential-difference equations, based on the expansion of the solution as a series of Fibonacci polynomials. Priyadarshana et al. [19] developed an efficient approximation technique known as the successive complementary expansion method (SCEM) for solving singularly perturbed differential-difference equations with mixed shifts. Kadalbajoo et al. [20] presented a comparative study of the fitted-mesh finite difference method, the B-spline collocation method, and the finite element method for a general singularly perturbed two-point boundary value problem. Mushahary et al. [21] constructed an upwind finite difference scheme on a Shishkin mesh for solving SPPDEs. To enhance convergence, the authors presented a hybrid finite difference scheme that employs the cubic spline difference method in the fine mesh regions and a midpoint upwind scheme in the coarse mesh regions. Rai and Sharma [22] developed an exponentially fitted finite difference approach to solving SPDDEs, adopting the Il'in-Allen-Southwell fitting technique. Senthilkumar et al. [23] presented an asymptotic streamline diffusion finite element method (SDFEM) for singularly perturbed convection-diffusion-type differential-difference equations. Liu and Xu [24] developed Galerkin methods based on Hermite splines for solving the singularly perturbed two-point boundary value problem of high-order elliptic differential equations. Constantinou and Xenophontos [25] presented finite element analysis on singularly perturbed problems. An exponentially graded mesh is initially implemented on reaction-diffusion problem with Galerkin finite element method, followed by solution of the convection-diffusion problem. Swamy et al. [26] adopted Galerkin method to solve singularly perturbed differential-difference equations with delay and advance shifts using fitting factor.

The numerical methods for solving singular perturbation problems typical may not provide stable solutions, due to the smaller values of the perturbation parameter ϵ. Hence, developing high accurate numerical methods for such problems for smaller values of ϵ is a challenging task. It is known that the finite element methods using exponential elements on non-uniform grids can condense in the boundary layers and produce good results. In this paper, we present fitted operator numerical scheme based on Galerkin finite element method with cubic Hermite shape functions for solving a boundary value problem of a singularly perturbed differential-difference equation with both delay (δ) and advance (η) parameters. Also we presented a finite element method on a piecewise-uniform mesh with cubic Hermite shape functions. The solutions obtained by both these methods are compared and the efficiency of the methods is illustrated.

The structure of the paper is as follows: In Section 2, we present the problem under consideration and discuss some properties of the solution. In Section 3, we derive numerical schemes using the fitted operator finite element method and the fitted mesh finite element method, employing cubic Hermite shape functions. Convergence analysis for these methods is detailed in Section 4. In Section 5, the computational results and graphs for the test problems are shown. Discussion and conclusions are followed in Section 6.

2. Statement of the Problem

We consider the SPDDE that incorporates both types of shifts as defined by

$$\epsilon u''(t) + a(t)u'(t) + \alpha(t)u(t-\delta) + \omega(t)u(t) + \beta(t)u(t+\eta) = f(t) \tag{2.1}$$

on $t \in (0,1), 0 < \epsilon \ll 1$, under the interval and boundary conditions

$$u(t) = \begin{cases} \phi(t); & t \in [-\delta, 0], \\ \chi(t); & t \in [1, 1+\eta], \end{cases} \tag{2.2}$$

where $0 < \epsilon \ll 1$ is the perturbation parameter, $a(t), \alpha(t), \omega(t), \beta(t), f(t)$, $\phi(t)$ and $\chi(t)$ are smooth functions and δ is the delay (negative shift) parameter and η is the advance (positive shift) parameter. As $\delta, \eta < \epsilon$, for $a(t) \geq M > 0$, $a(t) - \delta\alpha(t) + \eta\beta(t) > 0$, $\forall\, t \in [0,1]$ the solution exhibits a boundary layer near $t = 0$, while for $a(t) \leq \overline{M} < 0$, the solution exhibits a boundary layer near $t = 1$. Here we assume that $\alpha(t) \leq M_1$ and $\beta(t) \leq M_2$, $\alpha + \omega + \beta \leq -\mathscr{M}$ and the function $u(t)$ satisfies (2.1-2.2), it provides a smooth solution for (2.1) and (2.2) as it is both continuously differentiable in $(0,1)$ and continuous in the underlying interval $[0,1]$.

Since the solution of $u(t)$ of (2.1) and (2.2) is sufficiently differentiable, we expand the terms $u(t-\delta)$ and $u(t-\eta)$ using taylor series to obtain:

$$\begin{aligned} u(t-\delta) &\approx u(t) - \delta u'(t) + \frac{\delta^2}{2}u''(t) + O(\delta^3), \\ u(t+\eta) &\approx u(t) + \eta u'(t) + \frac{\eta^2}{2}u''(t) + O(\eta^3). \end{aligned} \tag{2.3}$$

By substituting Eq. (2.3) in Eq.(2.1), we obtain

$$\mathscr{L}(\mathcal{U}(t)) \equiv \mu\mathcal{U}''(t) + p(t)\mathcal{U}'(t) + q(t)\mathcal{U}(t) = r(t), 0 \leq t \leq 1 \tag{2.4}$$

subject to the conditions

$$\begin{aligned} \mathcal{U}(0) &= \phi(0) = \phi_0, \\ \mathcal{U}(1) &= \chi(1) = \chi_1. \end{aligned} \tag{2.5}$$

where $\mathcal{U}(t) \approx u(t)$, $\mu(t) = \epsilon + \alpha(t)\frac{\delta^2}{2} + \beta(t)\frac{\eta^2}{2}$, $p(t) = a(t) - \delta\alpha(t) + \eta\beta(t)$, $q(t) = \alpha(t) + \omega(t) + \beta(t)$ and $r(t) = f(t)$.

2.1. Some properties of the solution to the continuous problem.

The following lemma suggests that $\mathscr{L}$ in Eq. (2.4) follows minimum principle:

Lemma 2.1 *Suppose $\mathcal{U}(t)$ is a sufficiently smooth function, satisfying $\{\mathcal{U}(0), \mathcal{U}(1) \geq 0\}$, then $\mathcal{U}(t) \geq 0$, $0 \leq t \leq 1$, whenever $\mathscr{L}(\mathcal{U}(t)) \leq 0$, $0 \leq t \leq 1$.*

Proof: *Reader can refer [8] for the proof.* □

Lemma 2.2 *If $\mathcal{U}(t)$ is the solution of the problem (2.4) and (2.5), then we have $\|\mathcal{U}\| \leq \mathscr{M}^{-1}\|r\| + \max(|\phi_0|, |\chi_1|)$, where $\|.\|$ is the l_∞ norm given by $\|\mathcal{U}\| = \max_{t\in[0,1]} |\mathcal{U}(t)|$.*

Proof: *Reader can refer [8] for the proof.* □

Lemma 2.3 *Let the zeroth order approximate solution to (2.4) and (2.5) be $\mathcal{U}(t) = \mathcal{U}_0^o + \mathcal{U}_0^i$, where $\mathcal{U}_0^o$ is the approximate solution in the outer region of zeroth order and that in the layer region be $\mathcal{U}_0^i$. Then for a fixed positive integer j,*

$$\lim_{\mathtt{h}\to 0} \mathcal{U}(j\mathtt{h}) \approx \mathcal{U}_0^o(0) + (\phi(0) - \mathcal{U}_0^o(0))e^{-p(0)j\rho}, \rho = \frac{\mathtt{h}}{\mu(0)}$$

Proof: *Reader can refer [8] for the proof.* □

3. Numerical Methods

In this section, we propose the fitted operator and the fitted mesh finite element methods for the problem (2.4)-(2.5).

3.1. Fitted Operator Finite Element Method [FOFEM] via cubic Hermite shape functions

The domain $[0,1]$ is divided into $N+1$ non-overlapping intervals $0 = t_0, t_1 = \mathtt{h}, t_2 = 2\mathtt{h}, \cdots, t_n = j\mathtt{h}, \cdots, t_{N+1} = (N+1)\mathtt{h} = 1$, with a uniform mesh of size $\mathtt{h}$ for each interval.

The grid points $t_i, i = 0, 1, \cdots N+1$ can be determined by selecting the set of basis functions $\gamma_j(t)$, where $j = 0, 1, \cdots, N$. The cubic hermite shape functions are chosen to be $l_i(t)$, which are given as below for local coordinates $-1 \leq \check{\vartheta} \leq 1$:

$$
\begin{aligned}
l_0(\check{\vartheta}) &= \frac{1}{4}\left(2 - 3\check{\vartheta} + \check{\vartheta}^3\right) = \frac{1}{4}(1-\check{\vartheta})^2(2+\check{\vartheta}),\\
l_1(\check{\vartheta}) &= \frac{1}{4}\left(2 + 3\check{\vartheta} - \check{\vartheta}^3\right) = \frac{1}{4}(1+\check{\vartheta})^2(2-\check{\vartheta}),\\
l_2(\check{\vartheta}) &= \frac{\mathtt{h}}{8}\left(1 - \check{\vartheta} - \check{\vartheta}^2 + \check{\vartheta}^3\right) = \frac{\mathtt{h}}{8}(1-\check{\vartheta}^2)(1-\check{\vartheta}),\\
l_3(\check{\vartheta}) &= \frac{\mathtt{h}}{8}\left(-1 - \check{\vartheta} + \check{\vartheta}^2 + \check{\vartheta}^3\right) = -\frac{\mathtt{h}}{8}(1-\check{\vartheta}^2)(1+\check{\vartheta}).
\end{aligned}
\tag{3.1}
$$

Using these shape functions, the solution $\mathcal{U}$ at the interior nodes $t_1, t_2, \cdots, t_N$ can be obtained. At the end nodes t_0 and t_{N+1}, the solution $\mathcal{U}(t)$ is determined by imposing the given boundary conditions.

The integral equations obtained using the Galerkin method, are given below:

$$\left(\mu(t)\mathcal{U}''(t) + p(t)\mathcal{U}'(t) + q(t)\mathcal{U}(t), \gamma_j\right) = \left(r(t), \gamma_j\right), \ j = 1, 2, \cdots, N. \tag{3.2}$$

This represents an integral equation

$$\int_{t_0}^{t_N} \left(\mu(t)\mathcal{U}''(t) + p(t)\mathcal{U}'(t) + q(t)\mathcal{U}(t)\right)\gamma_j dt = \int_{t_0}^{t_N} r(t)\gamma_j dt. \tag{3.3}$$

Applying integrating by parts on (3.3) gives

$$-\left(\mu\frac{d\mathcal{U}}{dt}, \frac{d\gamma_j}{dt}\right) + \left(p(t)\frac{d\mathcal{U}}{dt} + q(t)\mathcal{U}, \gamma_j\right) + \left(\mu\frac{d\mathcal{U}}{dt}\gamma_j\right)_0^1 = \left(r(t), \gamma_j\right) \tag{3.4}$$

Substituting the trial function $\mathcal{U}(t) = \gamma_0(t) + \sum_{i=1}^{N} \mathcal{U}_i \gamma_j(t)$ into Eq. (3.4) yields

$$
\begin{aligned}
\sum_{i=1}^{N} \mathcal{U}_i \left(\mu\frac{d\gamma_i}{dt}, \frac{d\gamma_j}{dt}\right) - \sum_{i=1}^{N} \mathcal{U}_i \left(p(t)\frac{d\gamma_i}{dt} + q(t)\gamma_i, \gamma_j\right) = &\\
&- \phi_0\left(\frac{dl_0}{dt}, \frac{d\gamma_j}{dt}\right) - \chi_1\left(\frac{dl_{N+1}}{dt}, \frac{d\gamma_j}{dt}\right)\\
&+ \phi_0\left(p(t)\frac{dl_0}{dt} + q(t)l_0, \gamma_j\right) + \left(\mu\frac{d\mathcal{U}}{dt}, \gamma_j\right)_0^1 - \left(r(t), \gamma_j\right)\\
&+ \chi_1\left(p(t)\frac{dl_{N+1}}{dt} + q(t)l_{N+1}, \gamma_j\right), 1 \leq j \leq N.
\end{aligned}
\tag{3.5}
$$

The right side of Eq. (3.5) can be approximated with known boundary data, resulting N equations for values t_i that are not known at interior nodes.
Utilizing local coordinate system $(\check{\vartheta})$, the integrals in equation Eq. (3.5) can be evaluated.

Since $t = \frac{\mathtt{h}}{2}\check{\vartheta} + \frac{1}{2}$ and $\frac{d\check{\vartheta}}{dt} = \frac{2}{\mathtt{h}}$, we have, through simple integration,

$$
\begin{aligned}
\int_0^1 \frac{d\gamma_i}{dt}\frac{d\gamma_j}{dt}dt &= \int_{-1}^1 \frac{dl_0}{d\check{\vartheta}}\frac{d\check{\vartheta}}{dt}\frac{dl_1}{d\check{\vartheta}}\frac{d\check{\vartheta}}{dt}\frac{\mathtt{h}}{2}d\check{\vartheta} + \int_{-1}^1 \frac{dl_0}{d\check{\vartheta}}\frac{d\check{\vartheta}}{dt}\frac{dl_2}{d\check{\vartheta}}\frac{d\check{\vartheta}}{dt}\frac{\mathtt{h}}{2}d\check{\vartheta} + \int_{-1}^1 \frac{dl_0}{d\check{\vartheta}}\frac{d\check{\vartheta}}{dt}\frac{dl_3}{d\check{\vartheta}}\frac{d\check{\vartheta}}{dt}\frac{\mathtt{h}}{2}d\check{\vartheta} \\
&\quad + \int_{-1}^1 \frac{dl_1}{d\check{\vartheta}}\frac{d\check{\vartheta}}{dt}\frac{dl_2}{d\check{\vartheta}}\frac{d\check{\vartheta}}{dt}\frac{\mathtt{h}}{2}d\check{\vartheta} + \int_{-1}^1 \frac{dl_1}{d\check{\vartheta}}\frac{d\check{\vartheta}}{dt}\frac{dl_3}{d\check{\vartheta}}\frac{d\check{\vartheta}}{dt}\frac{\mathtt{h}}{2}d\check{\vartheta} + \int_{-1}^1 \frac{dl_2}{d\check{\vartheta}}\frac{d\check{\vartheta}}{dt}\frac{dl_3}{d\check{\vartheta}}\frac{d\check{\vartheta}}{dt}\frac{\mathtt{h}}{2}d\check{\vartheta} \\
&= \frac{6\mu}{5\mathtt{h}} + \frac{\mu\mathtt{h}}{30}, \text{ for } i = j-1, \\
\int_0^1 \frac{d\gamma_i}{dt}\frac{d\gamma_j}{dt}dt &= \int_{-1}^1 \frac{dl_0}{d\check{\vartheta}}\frac{d\check{\vartheta}}{dt}\frac{dl_0}{d\check{\vartheta}}\frac{d\check{\vartheta}}{dt}\frac{\mathtt{h}}{2}d\check{\vartheta} + \int_{-1}^1 \frac{dl_1}{d\check{\vartheta}}\frac{d\check{\vartheta}}{dt}\frac{dl_1}{d\check{\vartheta}}\frac{d\check{\vartheta}}{dt}\frac{\mathtt{h}}{2}d\check{\vartheta} + \int_{-1}^1 \frac{dl_2}{d\check{\vartheta}}\frac{d\check{\vartheta}}{dt}\frac{dl_2}{d\check{\vartheta}}\frac{d\check{\vartheta}}{dt}\frac{\mathtt{h}}{2}d\check{\vartheta} \\
&\quad + \int_{-1}^1 \frac{dl_3}{d\check{\vartheta}}\frac{d\check{\vartheta}}{dt}\frac{dl_3}{d\check{\vartheta}}\frac{d\check{\vartheta}}{dt}\frac{\mathtt{h}}{2}d\check{\vartheta} \\
&= \frac{-12\mu}{5\mathtt{h}} - \frac{4\mu\mathtt{h}}{15}, \text{ for } i = j, \\
\int_0^1 \frac{d\gamma_i}{dt}\frac{d\gamma_j}{dt}dt &= \int_{-1}^1 \frac{dl_1}{d\check{\vartheta}}\frac{d\check{\vartheta}}{dt}\frac{dl_0}{d\check{\vartheta}}\frac{d\check{\vartheta}}{dt}\frac{\mathtt{h}}{2}d\check{\vartheta} + \int_{-1}^1 \frac{dl_2}{d\check{\vartheta}}\frac{d\check{\vartheta}}{dt}\frac{dl_0}{d\check{\vartheta}}\frac{d\check{\vartheta}}{dt}\frac{\mathtt{h}}{2}d\check{\vartheta} + \int_{-1}^1 \frac{dl_3}{d\check{\vartheta}}\frac{d\check{\vartheta}}{dt}\frac{dl_0}{d\check{\vartheta}}\frac{d\check{\vartheta}}{dt}\frac{\mathtt{h}}{2}d\check{\vartheta} \\
&\quad + \int_{-1}^1 \frac{dl_2}{d\check{\vartheta}}\frac{d\check{\vartheta}}{dt}\frac{dl_1}{d\check{\vartheta}}\frac{d\check{\vartheta}}{dt}\frac{\mathtt{h}}{2}d\check{\vartheta} + \int_{-1}^1 \frac{dl_3}{d\check{\vartheta}}\frac{d\check{\vartheta}}{dt}\frac{dl_1}{d\check{\vartheta}}\frac{d\check{\vartheta}}{dt}\frac{\mathtt{h}}{2}d\check{\vartheta} + \int_{-1}^1 \frac{dl_3}{d\check{\vartheta}}\frac{d\check{\vartheta}}{dt}\frac{dl_2}{d\check{\vartheta}}\frac{d\check{\vartheta}}{dt}\frac{\mathtt{h}}{2}d\check{\vartheta} \\
&= \frac{6\mu}{5\mathtt{h}} + \frac{\mu\mathtt{h}}{30}, \text{ for } i = j+1, \\
\int_0^1 \frac{d\gamma_i}{dt}\frac{d\gamma_j}{dt}dt &= 0 \text{ for } |i-j| > 1.
\end{aligned}
$$

Assuming $p(t)$, $q(t)$, and $r(t)$ as constants, the integral equation Eq. (3.5) for a typical internal node j, takes the form

$$
\begin{aligned}
\left(\frac{6\mu}{5\mathtt{h}} + \frac{\mu\mathtt{h}}{30} + \frac{\mathtt{h}^2 p}{60} - \frac{p}{2} + \frac{9q\mathtt{h}}{70} - \frac{q\mathtt{h}^3}{140}\right)\mathcal{U}_{j-1} + \left(\frac{-12\mu}{5\mathtt{h}} - \frac{4\mu\mathtt{h}}{15} + \frac{26q\mathtt{h}}{35} + \frac{2q\mathtt{h}^3}{105}\right)\mathcal{U}_j \\
+ \left(\frac{6\mu}{5\mathtt{h}} + \frac{\mu\mathtt{h}}{30} - \frac{\mathtt{h}^2 p}{60} + \frac{p}{2} + \frac{9q\mathtt{h}}{70} - \frac{q\mathtt{h}^3}{140}\right)\mathcal{U}_{j+1} = r_j\mathtt{h}.
\end{aligned}
\tag{3.6}
$$

Rearranging Eq. (3.6), we obtain the Galerkin difference scheme, which consists of difference equations, and including a fitting factor σ, we obtain:

$$
\begin{aligned}
&\mu\sigma\left[\frac{(36+\mathtt{h}^2)\mathcal{U}_{j-1} - (72+8\mathtt{h}^2)\mathcal{U}_j + (36+\mathtt{h}^2)\mathcal{U}_{j+1}}{30\mathtt{h}^2}\right] + p_j\left[\left(\frac{\mathtt{h}}{60} - \frac{1}{2\mathtt{h}}\right)\mathcal{U}_{j-1} - \left(\frac{\mathtt{h}}{60} - \frac{1}{2\mathtt{h}}\right)\mathcal{U}_{j+1}\right] \\
&+ q_j\left[\left(\frac{9}{70} - \frac{\mathtt{h}^2}{140}\right)\mathcal{U}_{j-1} + \left(\frac{26}{35} + \frac{2\mathtt{h}^2}{105}\right)\mathcal{U}_j + \left(\frac{9}{70} - \frac{\mathtt{h}^2}{140}\right)\mathcal{U}_{j+1}\right] = r_j \text{ for } 1 \le j \le N-1.
\end{aligned}
\tag{3.7}
$$

As such, σ is a fitting factor that must to be chosen so that the solution of Eq. (3.7) converges uniformly. Multiplying Eq. (3.7) by $\mathtt{h}$ and finding the limit as $\mathtt{h} \to 0$, we obtain

$$
\lim_{\mathtt{h}\to 0}\left[\frac{\sigma}{\rho}\left(\frac{6}{5}\mathcal{U}(j\mathtt{h}-\mathtt{h}) - \frac{12}{5}\mathcal{U}(j\mathtt{h}) + \frac{6}{5}\mathcal{U}(j\mathtt{h}+\mathtt{h})\right) - \frac{p_j}{2}\left(\mathcal{U}(j\mathtt{h}-\mathtt{h}) - \mathcal{U}(j\mathtt{h}+\mathtt{h})\right)\right] = 0. \tag{3.8}
$$

According to Lemma 2.3, Eq. (3.8) gives, $\sigma = \frac{5\rho}{12}p(0)\coth\left(\frac{p(0)\rho}{2}\right)$ where $\rho = \frac{\mathtt{h}}{\mu(0)}$. which represents a constant fitting factor. In general, we consider a variable fitting factor

$$
\sigma_j = \frac{5\rho_j}{12}p_j\coth\left(\frac{p_j\rho_j}{2}\right) \quad \text{where } \rho_j = \frac{\mathtt{h}}{\mu_j}.
$$

Eq. (3.7) yields a three-term recurrence relation as

$$\mathcal{E}_j\,\mathcal{U}_{j-1} + \mathcal{F}_j\,\mathcal{U}_j + \mathcal{G}_j\,\mathcal{U}_{j+1} = \mathcal{H}_j\ ,\ 1 \leq j \leq N-1, \tag{3.9}$$

where

$$\begin{aligned}
\mathcal{E}_j &= \left(\frac{6\mu\sigma}{5\mathtt{h}^2} + \frac{\mu\sigma}{30} + \frac{p\mathtt{h}}{60} - \frac{p}{2\mathtt{h}} + \frac{9q}{70} - \frac{q\mathtt{h}^2}{140}\right),\\
\mathcal{F}_j &= \left(\frac{-12\mu\sigma}{5\mathtt{h}^2} - \frac{4\mu\sigma}{15} + \frac{26q}{35} + \frac{2q\mathtt{h}^2}{105}\right),\\
\mathcal{G}_j &= \left(\frac{6\mu\sigma}{5\mathtt{h}^2} + \frac{\mu\sigma}{30} - \frac{p\mathtt{h}}{60} + \frac{p}{2\mathtt{h}} + \frac{9q}{70} - \frac{q\mathtt{h}^2}{140}\right),\\
\mathcal{H}_j &= r_j.
\end{aligned}$$

This tridiagonal system along with the boundary conditions (2.5) can be solved using Thomas Algorithm.

3.2. Fitted Mesh Finite Element Method [FMFEM] via cubic Hermite shape functions

The following section illustrates the grid-selection strategy for the computation of solution for the SPBVP (2.4)-(2.5).

3.2.1. Piecewise-uniform mesh. Since the boundary layer appears towards the left side of the solution domain $\mathcal{D} = [0,1]$, it is split into two subdomains $\mathcal{D}_1$ and $\mathcal{D}_2$, ensuring that $\mathcal{D} = \mathcal{D}_1 \cup \mathcal{D}_2 = [0,\tau] \cup [\tau,1]$, in which τ is the known as transition parameter that was placed around $t = 0$, given by

$$\tau = \min\left\{\frac{1}{2}, \epsilon\tau_0 \ln(N)\right\} \tag{3.10}$$

where N is the number of grid points belonging to the domain $\mathcal{D} = [0,1]$ and $\tau_0 \geq \frac{1}{|\mathscr{M}|}$. It is clear that for $\tau = \frac{1}{2}$, the mesh is uniform, otherwise the mesh condenses near the left boundary. It is assumed that $N = 2^m$, where $m \geq 2$ is an integer, which guarantees that there is atleast one point in the boundary layer region.
So, each of the domains $\mathcal{D}_1$ and $\mathcal{D}_2$ contain same number of grid points, equispaced in the respective subdomains and the grid points t_w are defined as follows:

$$t_w = \begin{cases} w\mathtt{h}_1 & \text{for } 0 \leq w \leq \frac{N}{2} \\ \tau + (w - \frac{N}{2})\mathtt{h}_2 & \text{for } \frac{N}{2} < w \leq N \end{cases} \tag{3.11}$$

where $\mathtt{h}_1 = \frac{2\tau}{N}$ and $\mathtt{h}_2 = \frac{2(1-\tau)}{N}$ on the domains $\mathcal{D}_1$ and $\mathcal{D}_2$ respectively.
Similarly, in the case when the boundary layer occurs at the right end of the solution domain $\mathcal{D}$, we divide into subdomains $\mathcal{D}_1^*$ and $\mathcal{D}_2^*$ such that $\mathcal{D} = \mathcal{D}_1^* \cup \mathcal{D}_2^* = [0, 1-\tau] \cup [1-\tau, 1]$, where τ is so-called the transition parameter and is located near the point $t = 1$. We consider equal number of grid points in each subdomain $\mathcal{D}_1$ and $\mathcal{D}_2$ and uniform partition over the respective subdomains with grid points t_w, defined by

$$t_w = \begin{cases} w\mathtt{h}_2 & \text{for } 0 \leq w \leq \frac{N}{2} \\ 1 - \tau + (w - \frac{N}{2})\mathtt{h}_1 & \text{for } \frac{N}{2} < w \leq N \end{cases}. \tag{3.12}$$

Now we show that $\mathscr{L}$ satisfies the discrete minimum principle:

Lemma 3.1 *If the mesh function $\mathcal{U}(t_w)$ satisfying $\mathcal{U}(t_0), \mathcal{U}(t_N) \geq 0$, then $\mathcal{U}(t_w) \geq 0, 0 \leq t_w \leq 1$ for $\mathscr{L}(\mathcal{U}(t_w)) \leq 0, 0 < t_w < 1$.*

Proof: *Reader can refer [5] for the proof.* □

Lemma 3.2 *Let $\mathcal{U}_w$ be any mesh function such that $\mathcal{U}_0 = \mathcal{U}_N = 0$. Then for all $0 \leq w \leq N$,*

$$\|\mathcal{U}_w\| \leq \mathscr{M}^{-1} \max_{1\leq w\leq N-1} |\mathscr{L}(\mathcal{U}_w)|$$

.

Proof: *Reader can refer [5] for the proof.* □

Lemma 3.3 $e^{-\mathcal{M}(1-t_w)/\left(\epsilon+\frac{\delta^2}{2}M_1+\frac{\eta^2}{2}M_2\right)} \leq \prod_{v=w+1}^{N}\left(1+\frac{\mathcal{M}\mathtt{h}_v}{\epsilon+\frac{\delta^2}{2}M_1+\frac{\eta^2}{2}M_2}\right)^{-1}$ *for each w.*

Proof: *Reader can refer [5] for the proof.* □

Lemma 3.4 *For $w = 0, 1, \cdots, N$, we set $R_w = \prod_{v=1}^{w}\left(1+\frac{\mathcal{M}\mathtt{h}_v}{\epsilon+\frac{\delta^2}{2}M_1+\frac{\eta^2}{2}M_2}\right)$, then for $w = 0, 1, \cdots, N-1$, we have*

$$\mathscr{L}R_w \geq \frac{C}{\max\{\epsilon+\frac{\delta^2}{2}M_1+\frac{\eta^2}{2}M_2, \mathtt{h}_w\}}R_w.$$

Proof: *Reader can refer [5] for the proof.* □

Lemma 3.5 *There exists a constant C such that $\prod_{v=w+1}^{N}\left(1+\frac{\mathcal{M}\mathtt{h}_v}{\epsilon+\frac{\delta^2}{2}M_1+\frac{\eta^2}{2}M_2}\right)^{-1} \leq CN^{-4(1-w/N)}$ for $N/2 \leq w \leq N$.*

Proof: *Reader can refer [5] for the proof.* □

3.2.2. Derivation of the Numerical Scheme. From 3.1, we have $t = \frac{\mathtt{h}_w}{2}\check{\vartheta} + \frac{1}{2}$ and $\frac{d\check{\vartheta}}{dt} = \frac{2}{\mathtt{h}_w}$, where $\mathtt{h}_w = t_w - t_{w-1}$, so that from Eq. (3.5) by simple integration,

$$\begin{aligned}
\int_0^1 \frac{d\gamma_i}{dt}\frac{d\gamma_j}{dt}dt &= \int_{-1}^1 \frac{dl_0}{d\check{\vartheta}}\frac{d\check{\vartheta}}{dt}\frac{dl_1}{d\check{\vartheta}}\frac{d\check{\vartheta}}{dt}\frac{\mathtt{h}_w}{2}d\check{\vartheta} + \int_{-1}^1 \frac{dl_0}{d\check{\vartheta}}\frac{d\check{\vartheta}}{dt}\frac{dl_2}{d\check{\vartheta}}\frac{d\check{\vartheta}}{dt}\frac{\mathtt{h}_w}{2}d\check{\vartheta} + \int_{-1}^1 \frac{dl_0}{d\check{\vartheta}}\frac{d\check{\vartheta}}{dt}\frac{dl_3}{d\check{\vartheta}}\frac{d\check{\vartheta}}{dt}\frac{\mathtt{h}_w}{2}d\check{\vartheta} \\
&+ \int_{-1}^1 \frac{dl_1}{d\check{\vartheta}}\frac{d\check{\vartheta}}{dt}\frac{dl_2}{d\check{\vartheta}}\frac{d\check{\vartheta}}{dt}\frac{\mathtt{h}_w}{2}d\check{\vartheta} + \int_{-1}^1 \frac{dl_1}{d\check{\vartheta}}\frac{d\check{\vartheta}}{dt}\frac{dl_3}{d\check{\vartheta}}\frac{d\check{\vartheta}}{dt}\frac{\mathtt{h}_w}{2}d\check{\vartheta} + \int_{-1}^1 \frac{dl_2}{d\check{\vartheta}}\frac{d\check{\vartheta}}{dt}\frac{dl_3}{d\check{\vartheta}}\frac{d\check{\vartheta}}{dt}\frac{\mathtt{h}_w}{2}d\check{\vartheta} \\
&= \frac{6\mu}{5\mathtt{h}_w} + \frac{\mu\mathtt{h}_w}{30}, \text{ for } i = j-1,
\end{aligned}$$

$$\begin{aligned}
\int_0^1 \frac{d\gamma_i}{dt}\frac{d\gamma_j}{dt}dt &= \int_{-1}^1 \frac{dl_0}{d\check{\vartheta}}\frac{d\check{\vartheta}}{dt}\frac{dl_0}{d\check{\vartheta}}\frac{d\check{\vartheta}}{dt}\frac{\mathtt{h}_w}{2}d\check{\vartheta} + \int_{-1}^1 \frac{dl_1}{d\check{\vartheta}}\frac{d\check{\vartheta}}{dt}\frac{dl_1}{d\check{\vartheta}}\frac{d\check{\vartheta}}{dt}\frac{\mathtt{h}_w}{2}d\check{\vartheta} + \int_{-1}^1 \frac{dl_2}{d\check{\vartheta}}\frac{d\check{\vartheta}}{dt}\frac{dl_2}{d\check{\vartheta}}\frac{d\check{\vartheta}}{dt}\frac{\mathtt{h}_w}{2}d\check{\vartheta} \\
&+ \int_{-1}^1 \frac{dl_3}{d\check{\vartheta}}\frac{d\check{\vartheta}}{dt}\frac{dl_3}{d\check{\vartheta}}\frac{d\check{\vartheta}}{dt}\frac{\mathtt{h}_w}{2}d\check{\vartheta} \\
&= \frac{-12\mu}{5\mathtt{h}_w} - \frac{8\mu\mathtt{h}_w}{30}, \text{ for } i = j,
\end{aligned}$$

$$\begin{aligned}
\int_0^1 \frac{d\gamma_i}{dt}\frac{d\gamma_j}{dt}dt &= \int_{-1}^1 \frac{dl_1}{d\check{\vartheta}}\frac{d\check{\vartheta}}{dt}\frac{dl_0}{d\check{\vartheta}}\frac{d\check{\vartheta}}{dt}\frac{\mathtt{h}_w}{2}d\check{\vartheta} + \int_{-1}^1 \frac{dl_2}{d\check{\vartheta}}\frac{d\check{\vartheta}}{dt}\frac{dl_0}{d\check{\vartheta}}\frac{d\check{\vartheta}}{dt}\frac{\mathtt{h}_w}{2}d\check{\vartheta} + \int_{-1}^1 \frac{dl_3}{d\check{\vartheta}}\frac{d\check{\vartheta}}{dt}\frac{dl_0}{d\check{\vartheta}}\frac{d\check{\vartheta}}{dt}\frac{\mathtt{h}_w}{2}d\check{\vartheta} \\
&+ \int_{-1}^1 \frac{dl_2}{d\check{\vartheta}}\frac{d\check{\vartheta}}{dt}\frac{dl_1}{d\check{\vartheta}}\frac{d\check{\vartheta}}{dt}\frac{\mathtt{h}_w}{2}d\check{\vartheta} + \int_{-1}^1 \frac{dl_3}{d\check{\vartheta}}\frac{d\check{\vartheta}}{dt}\frac{dl_1}{d\check{\vartheta}}\frac{d\check{\vartheta}}{dt}\frac{\mathtt{h}_w}{2}d\check{\vartheta} + \int_{-1}^1 \frac{dl_3}{d\check{\vartheta}}\frac{d\check{\vartheta}}{dt}\frac{dl_2}{d\check{\vartheta}}\frac{d\check{\vartheta}}{dt}\frac{\mathtt{h}_w}{2}d\check{\vartheta} \\
&= \frac{6\mu}{5\mathtt{h}_w} + \frac{\mu\mathtt{h}_w}{30}, \text{ for } i = j+1,
\end{aligned}$$

$$\int_0^1 \frac{d\gamma_i}{dt}\frac{d\gamma_j}{dt}dt = 0 \text{ for } |i-j| > 1.$$

From Eq. (3.5), we obtain the Galerkin three-term recurrence relation

$$\overline{\mathcal{E}}_j \mathcal{U}_{j-1} + \overline{\mathcal{F}}_j \mathcal{U}_j + \overline{\mathcal{G}}_j \mathcal{U}_{j+1} = \overline{\mathcal{H}}_j \ , \ 1 \leq j \leq N-1, \tag{3.13}$$

where

$$\begin{aligned}
\overline{\mathcal{E}}_j &= \left(\frac{6\mu}{5\mathrm{h}_w^2} + \frac{\mu}{30} + \frac{p\mathrm{h}_w}{60} - \frac{p}{2\mathrm{h}_w} + \frac{9q}{70} - \frac{q\mathrm{h}_w^2}{140} \right), \\
\overline{\mathcal{F}}_j &= \left(\frac{-12\mu}{5\mathrm{h}_w^2} - \frac{4\mu}{15} + \frac{26q}{35} + \frac{2q\mathrm{h}_w^2}{105} \right), \\
\overline{\mathcal{G}}_j &= \left(\frac{6\mu}{5\mathrm{h}_w^2} + \frac{\mu}{30} - \frac{p\mathrm{h}_w}{60} + \frac{p}{2\mathrm{h}_w} + \frac{9q}{70} - \frac{q\mathrm{h}_w^2}{140} \right), \\
\overline{\mathcal{H}}_j &= r_j.
\end{aligned}$$

4. Convergence Analysis

In this section, we perform the convergence analysis for the method outlined in Sect. 3.1. The tridiagonal system Eq. (3.9) can be expressed in matrix form as follows:

$$\mathcal{A}\mathcal{U} = \mathcal{C}, \tag{4.1}$$

in which $\mathcal{A} = m_{ij}$, $1 \leq i, j \leq N-1$ is a tridiagonal matrix of order $N-1$, with the diagonals

$$\begin{aligned}
m_{ii+1} &= \frac{6\mu\sigma}{5\mathrm{h}} + \frac{\mu\sigma\mathrm{h}}{30} + \frac{p\mathrm{h}^2}{60} - \frac{p}{2} + \frac{9q\mathrm{h}}{70} - \frac{q\mathrm{h}^3}{140}, \\
m_{ii} &= \frac{-12\mu\sigma}{5\mathrm{h}} - \frac{4\mu\sigma\mathrm{h}}{15} + \frac{26q\mathrm{h}}{35} + \frac{2q\mathrm{h}^3}{105}, \\
m_{ii-1} &= \frac{6\mu\sigma}{5\mathrm{h}} + \frac{\mu\sigma\mathrm{h}}{30} - \frac{p\mathrm{h}^2}{60} + \frac{p}{2} + \frac{9q\mathrm{h}}{70} - \frac{q\mathrm{h}^3}{140},
\end{aligned} \tag{4.2}$$

and column vector form, $\mathcal{C} = \mathtt{h}\mathcal{H}_i$, for $i = 1, 2, \cdots N-1$. The local truncation error associated with the above scheme is

$$\iota_i = \mathtt{h}^2 \left[q_i \mathcal{U}_i + \frac{29p_i}{30} \mathcal{U}_i' + \frac{17q_i}{140} \mathcal{U}_i'' \right] + O(\mathtt{h}^3). \tag{4.3}$$

and $\mathcal{U} = (u_0, u_1, \cdots, u_N)$.
Additionally, we have

$$\mathcal{A}\overline{\mathcal{U}} - \mathcal{T}(\mathtt{h}) = \mathcal{C}, \tag{4.4}$$

where $\overline{\mathcal{U}} = (\overline{u}_0, \overline{u}_1, \cdots, \overline{u}_N)$ represents the actual solution, whereas $\mathcal{T}(\mathtt{h}) = (\mathcal{T}_0(\mathtt{h}_0), \mathcal{T}_1(\mathtt{h}_1), \cdots, \mathcal{T}_N(\mathtt{h}_N))^T$ has a local truncation error.
From (4.1) and (4.4), we get

$$\mathcal{A}(\overline{\mathcal{U}} - \mathcal{U}) = \mathcal{T}(\mathtt{h}), \tag{4.5}$$

Accordingly, the error equation becomes

$$\mathcal{A}\mathcal{E} = \mathcal{T}(\mathtt{h}), \tag{4.6}$$

where $\mathcal{E} = \overline{\mathcal{U}} - \mathcal{U} = (\mathtt{e}_0, \mathtt{e}_1, \cdots, \mathtt{e}_N)$.
Assuming S_i, has to be the i^{th} row sum of matrix $\mathcal{A}$, we obtain

$$\begin{aligned}
\mathsf{S}_i &= \sum_{j=1}^{N-1} m_{ij} = -\frac{6\mu\sigma}{5\mathrm{h}} - \frac{7\mu\sigma\mathrm{h}}{30} - \frac{p\mathrm{h}^2}{30} + \frac{p}{2} + \frac{61q\mathrm{h}}{70} + \frac{q\mathrm{h}^3}{84}, \quad \text{for } i = 1, \\
\mathsf{S}_i &= \sum_{j=1}^{N-1} m_{ij} = \mathtt{h}\left(-\frac{6\mu\sigma}{30} + q + \frac{q^2}{210} \right) = \mathcal{B}_{i_0}, \quad \text{for } i = 2, 3, \cdots, N-2, \\
\mathsf{S}_i &= \sum_{j=1}^{N-1} m_{ij} = -\frac{6\mu\sigma}{5\mathrm{h}} - \frac{7\mu\sigma\mathrm{h}}{30} + \frac{p\mathrm{h}^2}{30} - \frac{p}{2} + \frac{61q\mathrm{h}}{70} + \frac{q\mathrm{h}^3}{84}, \quad \text{for } i = N-1.
\end{aligned} \tag{4.7}$$

Choosing a sufficiently small $\mathtt{h}$ proves the irreducibility and monotonicity of matrix $\mathcal{A}$ ([27], [28]). This leads to the existence of $\mathcal{A}^{-1}$ and the nonnegative character of its elements.
Accordingly, we derive from Eq. (4.6),

$$\mathcal{E} = \mathcal{A}^{-1}T(\mathtt{h}),$$
$$\|\mathcal{E}\| = \|\mathcal{A}^{-1}\| \cdot \|T(\mathtt{h})\|. \tag{4.8}$$

In addition, matrix theory provides

$$\sum_{i=1}^{N-1} \overline{m}_{k,i}\mathsf{S}_i = 1,\ k = 1(1)N-1, \tag{4.9}$$

in which for any i that ranges from 1 to $N-1$, $\overline{m}_{k,i}$ is (k,i) element associated with matrix $\mathcal{A}^{-1}$.
Thus,

$$\sum_{i=1}^{N-1} \overline{m}_{k,i} = \frac{1}{\min\limits_{1\le i\le N-1} \mathsf{S}_i} = \frac{1}{\mathcal{B}_{i_0}} \le \frac{1}{|\mathcal{B}_{i_0}|}. \tag{4.10}$$

We specify $\|\mathcal{A}^{-1}\| = \max\limits_{1\le k\le N-1} \sum\limits_{i=1}^{N-1} |\overline{m}_{k,i}|$ and $\|T(\mathtt{h})\| = \max\limits_{1\le i\le N-1} |T_i(\mathtt{h})|$.

From Eqs (4.3), (4.6), (4.8) and (4.10), we get $e_j = \sum\limits_{i=1}^{N-1} |\overline{m}_{k,i}| T_i(\mathtt{h}),\ j = 1(1)N-1$, which show that

$$e_j \le \frac{\mathtt{k}(\mathtt{h}^2)}{|\mathcal{B}_{i_0}|},\ j = 1(1)N-1,$$

where $\mathtt{k} = \left(q_i\mathcal{U}_i + \frac{29p_i}{30}\mathcal{U}_i' + \frac{17q_i}{140}\mathcal{U}_i'' \right)$.
Hence $\|\mathcal{E}\| = O(\mathtt{h})$. That is, when dealing with uniform mesh, our approach simplifies to a first-order convergent scheme (3.9).
Note: To validate the accuracy of the fitted mesh finite element method described in Sect. 3.2, we can adopt a convergence strategy as in [5], given by the following theorem:

Theorem 4.1 *$a(t), \alpha(t), \omega(t), \beta(t), f(t),\ \phi(t)$ and $\chi(t)$ be sufficiently smooth functions so that $\mathcal{U}(t) \in C^3[0,1]$. Let $\mathcal{U}_w,\ w = 0(1)N$ be the approximate solution of (2.4), obtained using fitted mesh finite element method (3.13) with the conditions (2.5). Then, there is a constant $\mathcal{M}$ independent of ϵ and the mesh size such that*

$$\sup_{0<\epsilon<<1} \max_{1\le w\le N-1} |\hat{\mathcal{U}}_w - \mathcal{U}_w| \le \mathcal{M}N^{-2}\ln^2 N.$$

5. Numerical Results

To analyze the efficacy of current methods, four problems of singularly perturbed linear differential equations with mixed shifts are examined. Two problems with solutions exhibiting boundary layer to the left of the interval [0,1] and two problems with right layer. Since the exact solutions for such problems with for various values of δ and η are unknown, the double mesh principle, as given below, is used to determine the maximum absolute errors:

$$E_N = \max_{0\le i\le N} |\mathcal{U}_i^N - \mathcal{U}_{2i}^{2N}|.$$

Tables 1-8 provide the maximum absolute errors and rate of convergence for the test problems that were considered with $\delta = \eta = 0.5\epsilon$. The graphical solutions for the examples, corresponding to various values of the shifts, are presented in Figs. (1-8). The numerical rate of convergence for all examples has been calculated using the formula

$$R_N = \frac{log|E_N/E_{2N}|}{log2}.$$

Example 5.1 $\epsilon u''(t) + u'(t) - 2u(t-\delta) + u(t) - u(t+\eta) = -1$, subject to the interval and boundary conditions $u(t) = 1; -\delta \le t \le 0, u(t) = 1, 1 \le t \le 1+\eta$.

Example 5.2 $\epsilon u''(t) + 2.5u'(t) - 2e^t u(t-\delta) - u(t) - tu(t+\eta) = 1$, subject to the interval and boundary conditions $u(t) = 1; -\delta \le t \le 0, u(t) = 1, 1 \le t \le 1+\eta$.

Example 5.3 $\epsilon u''(t) - u'(t) - 2u(t-\delta) + u(t) - 2u(t+\eta) = 0$, subject to the interval and boundary conditions $u(t) = 1; -\delta \le t \le 0, u(t) = -1, 1 \le t \le 1+\eta$.

Example 5.4 $\epsilon u''(t) - (1+e^{-t^2})u'(t) - tu(t-\delta) - t^2 u(t) - (1.5-e^{-t})u(t+\eta) = 0$, subject to the interval and boundary conditions $u(t) = 1; -\delta \le t \le 0, u(t) = 1, 1 \le t \le 1+\eta$.

6. Discussion and Conclusions

In this paper, numerical approaches based on the fitted operator finite element method [FOFEM] and the fitted mesh finite element method [FMFEM] via the Galerkin method are proposed for solving singularly perturbed boundary value problems for second-order ordinary differential equation with mixed shifts.The maximum absolute errors for the solution of the test problems are tabulated in Tables 1-4 and the rate of convergence for the problems for different values of ϵ are tabulated in Tables 5-8. From these numerical computations, it can be observed that the methods work well for problems with shifts smaller than the perturbation parameter. Also, the method [FOFEM] shows a first-order uniform rate of convergence, while method [FMFEM] shows an almost second-order uniform rate of convergence irrespective of the size of the perturbation parameter ϵ. The results are compared to that in [7] in tables 9-12, which show that the methods presented in this paper are in good agreement. The graphs for the solution of the test problems, for various values of δ and η are depicted in Figs. 1-8. These figures indicate that as the shifts increase in magnitude, the thickness of the boundary layer decreases when the solution demonstrates layer behavior near the left side of the underlying interval. Conversely, in the case of the right-end boundary layer, the thickness increases. The log-log plots depicted in Figs. 9 - 12 illustrate the expected numerical order of convergence for Examples 5.1-5.4. With the support of the extensive numerical results, we conclude that the approaches given in this paper provide a major contribution towards the solution of singularly perturbed linear boundary value problems with mixed shifts.

Table 1: Maximum absolute errors for Example 5.1 when $\delta = 0.5\epsilon$, $\eta = 0.5\epsilon$.

$\epsilon \downarrow N \rightarrow$	100	200	300	400	500
FOFEM					
10^{-1}	1.6064E-05	4.0100E-06	1.7817E-06	1.0021E-06	6.4133E-07
10^{-2}	2.4228E-04	5.4008E-05	2.3609E-05	1.3410E-05	8.5827E-06
10^{-3}	7.8771E-04	3.4219E-04	1.8403E-04	1.2151E-04	8.8285E-05
10^{-4}	7.9846E-04	4.0366E-04	2.7011E-04	2.0295E-04	1.6253E-04
10^{-5}	7.9846E-04	4.0366E-04	2.7011E-04	2.0296E-04	1.6255E-04
10^{-6}	7.9846E-04	4.0366E-04	2.7011E-04	2.0296E-04	1.6255E-04
10^{-7}	7.9846E-04	4.0366E-04	2.7011E-04	2.0296E-04	1.6255E-04
10^{-8}	7.9846E-04	4.0366E-04	2.7011E-04	2.0296E-04	1.6255E-04
10^{-9}	7.9846E-04	4.0366E-04	2.7011E-04	2.0296E-04	1.6255E-04
10^{-10}	7.9846E-04	4.0366E-04	2.7011E-04	2.0296E-04	1.6255E-04
FMFEM					
10^{-1}	8.5746E-05	2.1422E-05	9.5209E-06	5.3550E-06	3.4270E-06
10^{-2}	7.8031E-03	1.7930E-03	7.8525E-04	4.4281E-04	2.8342E-04
10^{-3}	2.0990E-02	6.0111E-03	2.9792E-03	1.8125E-03	1.2271E-03
10^{-4}	2.0890E-02	5.9630E-03	2.9474E-03	1.7900E-03	1.2080E-03
10^{-5}	2.0896E-02	5.9688E-03	2.9496E-03	1.7893E-03	1.2066E-03
10^{-6}	2.0892E-02	5.9685E-03	2.9531E-03	1.7937E-03	1.2114E-03
10^{-7}	2.0891E-02	5.9678E-03	2.9522E-03	1.7930E-03	1.2109E-03
10^{-8}	2.0891E-02	5.9677E-03	2.9520E-03	1.7928E-03	1.2106E-03
10^{-9}	2.0891E-02	5.9677E-03	2.9520E-03	1.7928E-03	1.2106E-03
10^{-10}	2.0891E-02	5.9677E-03	2.9520E-03	1.7928E-03	1.2106E-03

Table 2: Maximum absolute errors for Example 5.2 when $\delta = 0.5\epsilon$, $\eta = 0.5\epsilon$.

$\epsilon \downarrow N \rightarrow$	100	200	300	400	500
FOFEM					
10^{-1}	1.7664E-04	4.4234E-05	1.9666E-05	1.1063E-05	7.0808E-06
10^{-2}	1.8317E-03	5.0358E-04	2.2811E-04	1.2918E-04	8.2937E-05
10^{-3}	3.3232E-03	1.6786E-03	1.0942E-03	7.7708E-04	5.7660E-04
10^{-4}	3.3233E-03	1.6851E-03	1.1287E-03	8.4857E-04	6.7983E-04
10^{-5}	3.3233E-03	1.6851E-03	1.1287E-03	8.4857E-04	6.7983E-04
10^{-6}	3.3233E-03	1.6851E-03	1.1287E-03	8.4857E-04	6.7983E-04
10^{-7}	3.3233E-03	1.6851E-03	1.1287E-03	8.4857E-04	6.7983E-04
10^{-8}	3.3233E-03	1.6851E-03	1.1287E-03	8.4857E-04	6.7983E-04
10^{-9}	3.3233E-03	1.6851E-03	1.1287E-03	8.4857E-04	6.7983E-04
10^{-10}	3.3233E-03	1.6851E-03	1.1287E-03	8.4857E-04	6.7983E-04
FMFEM					
10^{-1}	1.1821E-03	2.9391E-04	1.3069E-04	7.3504E-05	4.7032E-05
10^{-2}	3.5310E-02	9.9038E-03	5.1690E-03	3.1485E-03	2.1599E-03
10^{-3}	3.4347E-02	9.5052E-03	4.9202E-03	2.9545E-03	2.0133E-03
10^{-4}	3.4318E-02	9.4730E-03	4.8947E-03	2.9341E-03	1.9980E-03
10^{-5}	3.4310E-02	9.4980E-03	4.9115E-03	2.9449E-03	2.0026E-03
10^{-6}	3.4305E-02	9.4930E-03	4.9106E-03	2.9482E-03	2.0083E-03
10^{-7}	3.4304E-02	9.4919E-03	4.9094E-03	2.9467E-03	2.0069E-03
10^{-8}	3.4304E-02	9.4918E-03	4.9093E-03	2.9465E-03	2.0067E-03
10^{-9}	3.4304E-02	9.4918E-03	4.9093E-03	2.9465E-03	2.0067E-03
10^{-10}	3.4304E-02	9.4918E-03	4.9093E-03	2.9465E-03	2.0067E-03

Table 3: Maximum absolute errors for Example 5.3 when $\delta = 0.5\epsilon$, $\eta = 0.5\epsilon$.

$\epsilon \downarrow N \rightarrow$	100	200	300	400	500
FOFEM					
10^{-1}	1.0129E-04	2.5300E-05	1.1243E-05	6.3242E-06	4.0475E-06
10^{-2}	1.3656E-03	3.1902E-04	1.4002E-04	7.8415E-05	5.0083E-05
10^{-3}	5.0251E-03	2.3009E-03	1.3203E-03	8.4083E-04	5.7166E-04
10^{-4}	5.0667E-03	2.5535E-03	1.7069E-03	1.2819E-03	1.0263E-03
10^{-5}	5.0667E-03	2.5535E-03	1.7069E-03	1.2819E-03	1.0264E-03
10^{-6}	5.0667E-03	2.5535E-03	1.7069E-03	1.2819E-03	1.0264E-03
10^{-7}	5.0667E-03	2.5535E-03	1.7069E-03	1.2819E-03	1.0264E-03
10^{-8}	5.0667E-03	2.5535E-03	1.7069E-03	1.2819E-03	1.0264E-03
10^{-9}	5.0667E-03	2.5535E-03	1.7069E-03	1.2819E-03	1.0264E-03
10^{-10}	5.0667E-03	2.5535E-03	1.7069E-03	1.2819E-03	1.0264E-03
FMFEM					
10^{-1}	2.3180E-04	5.7887E-05	2.5722E-05	1.4468E-05	9.2591E-06
10^{-2}	1.9203E-02	4.4110E-03	1.9317E-03	1.0876E-03	6.9631E-04
10^{-3}	2.0886E-02	6.3087E-03	3.1377E-03	1.9222E-03	1.3153E-03
10^{-4}	2.0767E-02	6.2654E-03	3.1113E-03	1.9029E-03	1.3001E-03
10^{-5}	2.0758E-02	6.2640E-03	3.1099E-03	1.9014E-03	1.2988E-03
10^{-6}	2.0756E-02	6.2636E-03	3.1106E-03	1.9023E-03	1.2997E-03
10^{-7}	2.0756E-02	6.2633E-03	3.1103E-03	1.9021E-03	1.2996E-03
10^{-8}	2.0756E-02	6.2633E-03	3.1103E-03	1.9021E-03	1.2995E-03
10^{-9}	2.0756E-02	6.2633E-03	3.1103E-03	1.9021E-03	1.2995E-03
10^{-10}	2.0756E-02	6.2633E-03	3.1102E-03	1.9021E-03	1.2995E-03

Table 4: Maximum absolute errors for Example 5.4 when $\delta = 0.5\epsilon$, $\eta = 0.5\epsilon$.

$\epsilon \downarrow N \rightarrow$	100	200	300	400	500
FOFEM					
10^{-1}	1.0078E-04	2.5188E-05	1.1195E-05	6.2959E-06	4.0295E-06
10^{-2}	1.3298E-03	2.9515E-04	1.3565E-04	7.5869E-05	4.8151E-05
10^{-3}	2.6654E-03	1.3195E-03	8.4129E-04	5.9236E-04	4.3850E-04
10^{-4}	2.6676E-03	1.3514E-03	9.0491E-04	6.8020E-04	5.4489E-04
10^{-5}	2.6676E-03	1.3514E-03	9.0491E-04	6.8020E-04	5.4489E-04
10^{-6}	2.6676E-03	1.3514E-03	9.0491E-04	6.8020E-04	5.4489E-04
10^{-7}	2.6676E-03	1.3514E-03	9.0491E-04	6.8020E-04	5.4489E-04
10^{-8}	2.6676E-03	1.3514E-03	9.0491E-04	6.8020E-04	5.4489E-04
10^{-9}	2.6676E-03	1.3514E-03	9.0491E-04	6.8020E-04	5.4489E-04
10^{-10}	2.6676E-03	1.3514E-03	9.0491E-04	6.8020E-04	5.4489E-04
FMFEM					
10^{-1}	3.6160E-04	9.0388E-05	4.0157E-05	2.2587E-05	1.4455E-05
10^{-2}	3.3804E-02	7.2761E-03	3.1548E-03	1.7683E-03	1.1337E-03
10^{-3}	8.9037E-02	2.8322E-02	1.3142E-02	8.1947E-03	5.6710E-03
10^{-4}	8.8699E-02	2.8554E-02	1.3302E-02	8.3783E-03	5.8062E-03
10^{-5}	8.8500E-02	2.8126E-02	1.3096E-02	8.2561E-03	5.7652E-03
10^{-6}	8.8598E-02	2.8177E-02	1.3069E-02	8.1452E-03	5.6338E-03
10^{-7}	8.8611E-02	2.8195E-02	1.3088E-02	8.1730E-03	5.6572E-03
10^{-8}	8.8612E-02	2.8197E-02	1.3090E-02	8.1772E-03	5.6618E-03
10^{-9}	8.8612E-02	2.8198E-02	1.3091E-02	8.1776E-03	5.6623E-03
10^{-10}	8.8612E-02	2.8197E-02	1.3091E-02	8.1776E-03	5.6623E-03

Table 5: Rate of convergence for Example 5.1 when $\delta = 0.5\epsilon$, $\eta = 0.5\epsilon$.

$\epsilon \downarrow N \rightarrow$	100	200	300	400	500
FOFEM					
10^{-1}	2.0022E+00	2.0005E+00	2.0002E+00	2.0001E+00	2.0001E+00
10^{-2}	2.1654E+00	2.0098E+00	1.9889E+00	2.0098E+00	2.0066E+00
10^{-3}	1.2029E+00	1.4938E+00	1.4796E+00	1.6250E+00	1.8076E+00
10^{-4}	9.8408E-01	9.9199E-01	9.9533E-01	1.0015E+00	1.0161E+00
10^{-5}	9.8408E-01	9.9198E-01	9.9464E-01	9.9597E-01	9.9677E-01
10^{-6}	9.8408E-01	9.9198E-01	9.9464E-01	9.9597E-01	9.9677E-01
10^{-7}	9.8408E-01	9.9198E-01	9.9464E-01	9.9597E-01	9.9677E-01
10^{-8}	9.8408E-01	9.9198E-01	9.9464E-01	9.9597E-01	9.9677E-01
10^{-9}	9.8408E-01	9.9198E-01	9.9464E-01	9.9597E-01	9.9677E-01
10^{-10}	9.8408E-01	9.9198E-01	9.9464E-01	9.9597E-01	9.9677E-01
FMFEM					
10^{-1}	2.0010E+00	2.0001E+00	2.0002E+00	2.0001E+00	2.0000E+00
10^{-2}	2.1217E+00	2.0176E+00	1.9972E+00	2.0033E+00	2.0042E+00
10^{-3}	1.8040E+00	1.7297E+00	1.7299E+00	1.7410E+00	1.7503E+00
10^{-4}	1.8087E+00	1.7360E+00	1.7392E+00	1.7547E+00	1.7666E+00
10^{-5}	1.8077E+00	1.7380E+00	1.7425E+00	1.7573E+00	1.7687E+00
10^{-6}	1.8075E+00	1.7344E+00	1.7382E+00	1.7547E+00	1.7696E+00
10^{-7}	1.8076E+00	1.7348E+00	1.7380E+00	1.7524E+00	1.7639E+00
10^{-8}	1.8076E+00	1.7350E+00	1.7383E+00	1.7530E+00	1.7648E+00
10^{-9}	1.8076E+00	1.7350E+00	1.7383E+00	1.7531E+00	1.7650E+00
10^{-10}	1.8076E+00	1.7350E+00	1.7384E+00	1.7531E+00	1.7650E+00

Table 6: Rate of convergence for Example 5.2 when $\delta = 0.5\epsilon$, $\eta = 0.5\epsilon$.

$\epsilon \downarrow N \rightarrow$	100	200	300	400	500
FOFEM					
10^{-1}	1.9976E+00	1.9994E+00	1.9997E+00	1.9999E+00	1.9999E+00
10^{-2}	1.8629E+00	1.9628E+00	1.9832E+00	1.9905E+00	1.9939E+00
10^{-3}	9.8534E-01	1.1111E+00	1.3098E+00	1.4824E+00	1.6097E+00
10^{-4}	9.7977E-01	9.8972E-01	9.9310E-01	9.9481E-01	9.9585E-01
10^{-5}	9.7977E-01	9.8972E-01	9.9310E-01	9.9481E-01	9.9584E-01
10^{-6}	9.7977E-01	9.8972E-01	9.9310E-01	9.9481E-01	9.9584E-01
10^{-7}	9.7977E-01	9.8972E-01	9.9310E-01	9.9481E-01	9.9584E-01
10^{-8}	9.7977E-01	9.8972E-01	9.9310E-01	9.9481E-01	9.9584E-01
10^{-9}	9.7977E-01	9.8972E-01	9.9310E-01	9.9481E-01	9.9584E-01
10^{-10}	9.7977E-01	9.8972E-01	9.9310E-01	9.9481E-01	9.9584E-01
FMFEM					
10^{-1}	2.0079E+00	1.9995E+00	2.0009E+00	2.0005E+00	2.0003E+00
10^{-2}	1.8340E+00	1.6533E+00	1.7067E+00	1.7012E+00	1.7106E+00
10^{-3}	1.8534E+00	1.6858E+00	1.7583E+00	1.7628E+00	1.7934E+00
10^{-4}	1.8571E+00	1.6909E+00	1.7643E+00	1.7701E+00	1.8028E+00
10^{-5}	1.8529E+00	1.6894E+00	1.7673E+00	1.7760E+00	1.8079E+00
10^{-6}	1.8535E+00	1.6870E+00	1.7595E+00	1.7652E+00	1.7980E+00
10^{-7}	1.8536E+00	1.6876E+00	1.7605E+00	1.7659E+00	1.7972E+00
10^{-8}	1.8536E+00	1.6877E+00	1.7607E+00	1.7664E+00	1.7980E+00
10^{-9}	1.8536E+00	1.6877E+00	1.7608E+00	1.7664E+00	1.7981E+00
10^{-10}	1.8536E+00	1.6877E+00	1.7608E+00	1.7664E+00	1.7981E+00

Table 7: Rate of convergence for Example 5.3 when $\delta = 0.5\epsilon$, $\eta = 0.5\epsilon$.

$\epsilon \downarrow N \rightarrow$	100	200	300	400	500
FOFEM					
10^{-1}	2.0013E+00	2.0002E+00	2.0000E+00	2.0000E+00	2.0000E+00
10^{-2}	2.0978E+00	2.0245E+00	2.0109E+00	2.0053E+00	2.0018E+00
10^{-3}	1.1269E+00	1.4523E+00	1.6973E+00	1.8827E+00	2.0262E+00
10^{-4}	9.8855E-01	9.9419E-01	9.9652E-01	1.0004E+00	1.0094E+00
10^{-5}	9.8855E-01	9.9419E-01	9.9610E-01	9.9707E-01	9.9765E-01
10^{-6}	9.8855E-01	9.9419E-01	9.9610E-01	9.9707E-01	9.9765E-01
10^{-7}	9.8855E-01	9.9419E-01	9.9610E-01	9.9707E-01	9.9765E-01
10^{-8}	9.8855E-01	9.9419E-01	9.9610E-01	9.9707E-01	9.9765E-01
10^{-9}	9.8855E-01	9.9419E-01	9.9610E-01	9.9707E-01	9.9765E-01
10^{-10}	9.8855E-01	9.9419E-01	9.9610E-01	9.9707E-01	9.9765E-01
FMFEM					
10^{-1}	2.0016E+00	2.0004E+00	2.0002E+00	2.0001E+00	2.0001E+00
10^{-2}	2.1222E+00	2.0200E+00	1.9988E+00	2.0022E+00	2.0042E+00
10^{-3}	1.7271E+00	1.7146E+00	1.7152E+00	1.7327E+00	1.7563E+00
10^{-4}	1.7288E+00	1.7192E+00	1.7221E+00	1.7414E+00	1.7669E+00
10^{-5}	1.7285E+00	1.7200E+00	1.7234E+00	1.7426E+00	1.7681E+00
10^{-6}	1.7285E+00	1.7192E+00	1.7223E+00	1.7420E+00	1.7683E+00
10^{-7}	1.7285E+00	1.7193E+00	1.7223E+00	1.7415E+00	1.7671E+00
10^{-8}	1.7285E+00	1.7194E+00	1.7223E+00	1.7416E+00	1.7673E+00
10^{-9}	1.7285E+00	1.7194E+00	1.7224E+00	1.7417E+00	1.7673E+00
10^{-10}	1.7285E+00	1.7193E+00	1.7223E+00	1.7417E+00	1.7673E+00

Table 8: Rate of convergence for Example 5.4 when $\delta = 0.5\epsilon$, $\eta = 0.5\epsilon$.

$\epsilon \downarrow N \rightarrow$	100	200	300	400	500
FOFEM					
10^{-1}	2.0005E+00	2.0002E+00	2.0002E+00	2.0000E+00	2.0001E+00
10^{-2}	2.1717E+00	1.9599E+00	2.0195E+00	2.0109E+00	1.9997E+00
10^{-3}	1.0144E+00	1.1555E+00	1.3295E+00	1.5115E+00	1.6758E+00
10^{-4}	9.8115E-01	9.9039E-01	9.9356E-01	9.9537E-01	9.9734E-01
10^{-5}	9.8115E-01	9.9039E-01	9.9355E-01	9.9514E-01	9.9611E-01
10^{-6}	9.8115E-01	9.9039E-01	9.9355E-01	9.9514E-01	9.9611E-01
10^{-7}	9.8115E-01	9.9039E-01	9.9355E-01	9.9514E-01	9.9611E-01
10^{-8}	9.8115E-01	9.9039E-01	9.9355E-01	9.9514E-01	9.9611E-01
10^{-9}	9.8115E-01	9.9039E-01	9.9355E-01	9.9514E-01	9.9611E-01
10^{-10}	9.8115E-01	9.9039E-01	9.9355E-01	9.9514E-01	9.9611E-01
FMFEM					
10^{-1}	2.0002E+00	2.0006E+00	2.0002E+00	2.0001E+00	2.0001E+00
10^{-2}	2.2159E+00	2.0408E+00	2.0031E+00	2.0010E+00	2.0065E+00
10^{-3}	1.6525E+00	1.7892E+00	1.6807E+00	1.6660E+00	1.6657E+00
10^{-4}	1.6352E+00	1.7689E+00	1.6506E+00	1.6469E+00	1.6348E+00
10^{-5}	1.6538E+00	1.7684E+00	1.6315E+00	1.6217E+00	1.6181E+00
10^{-6}	1.6527E+00	1.7905E+00	1.6820E+00	1.6610E+00	1.6455E+00
10^{-7}	1.6520E+00	1.7865E+00	1.6765E+00	1.6639E+00	1.6632E+00
10^{-8}	1.6519E+00	1.7859E+00	1.6746E+00	1.6610E+00	1.6580E+00
10^{-9}	1.6519E+00	1.7858E+00	1.6744E+00	1.6606E+00	1.6573E+00
10^{-10}	1.6519E+00	1.7858E+00	1.6744E+00	1.6606E+00	1.6572E+00

Table 9: Example 5.1 with $\delta = 0.5\epsilon$, $\eta = 0.5\epsilon$.

$\epsilon \downarrow N \rightarrow$	2^5	2^6	2^7	2^8	2^9	2^{10}
Maximum absolute errors using FOFEM						
2^{-1}	1.7258E-05	4.3103E-06	1.0778E-06	2.6944E-07	6.7375E-08	1.6731E-08
2^{-3}	1.1911E-04	2.9637E-05	7.4069E-06	1.8510E-06	4.6277E-07	1.1570E-07
2^{-5}	6.9521E-04	1.5340E-04	3.8675E-05	9.5949E-06	2.3941E-06	5.9858E-07
2^{-7}	1.8014E-03	6.5753E-04	1.9109E-04	4.2642E-05	1.0571E-05	2.6273E-06
2^{-9}	2.3814E-03	1.1876E-03	4.7642E-04	1.7126E-04	4.9043E-05	1.0974E-05
E_N	2.3814E-03	1.1876E-03	4.7642E-04	1.7126E-04	4.9043E-05	1.0974E-05
R_N	1.0038	1.3177	1.4761	1.8041	1.9993	1.9306
E_N [7]	2.7451E-03	1.3536E-03	5.4069E-04	1.6480E-04	4.3735E-05	1.1107E-05
R_N [7]	1.0201	1.3239	1.7141	1.9139	1.9941	

Table 10: Example 5.2 with $\delta = 0.5\epsilon$, $\eta = 0.5\epsilon$.

$\epsilon \downarrow N \rightarrow$	2^5	2^6	2^7	2^8	2^9	2^{10}
Maximum absolute errors using FOFEM						
2^{-1}	1.2195E-04	3.0464E-05	7.6145E-06	1.9036E-06	4.7590E-07	1.1899E-07
2^{-3}	7.5874E-04	1.8993E-04	4.7413E-05	1.1849E-05	2.9620E-06	7.4050E-07
2^{-5}	4.0403E-03	9.3834E-04	2.3035E-04	5.7327E-05	1.4315E-05	3.5786E-06
2^{-7}	1.2796E-02	4.3355E-03	1.0737E-03	2.5098E-04	6.1699E-05	1.5376E-05
2^{-9}	1.5328E-02	7.6725E-03	3.3247E-03	1.1117E-03	2.7327E-04	6.3985E-05
E_N	1.5328E-02	7.6725E-03	3.3247E-03	1.1117E-03	2.7327E-04	6.3985E-05
R_N	0.9984	1.2065	1.5804	1.9998	1.9997	1.9652
E_N [7]	1.0119E-02	5.2286E-03	2.6240E-03	1.1382E-03	3.7365E-04	1.0212E-04
R_N [7]	0.9526	0.9947	1.2050	1.6070	1.8714	

Table 11: Example 5.3 with $\delta = 0.5\epsilon$, $\eta = 0.5\epsilon$.

$\epsilon \downarrow N \rightarrow$	2^5	2^6	2^7	2^8	2^9	2^{10}
Maximum absolute errors using FMFEM						
2^{-1}	7.5721E-04	1.8952E-04	4.7322E-05	1.1827E-05	2.9565E-06	7.3913E-07
2^{-3}	7.7441E-03	1.9027E-03	4.7249E-04	1.1806E-04	2.9498E-05	7.3744E-06
2^{-5}	1.2902E-01	3.2238E-02	7.0805E-03	1.7190E-03	4.2750E-04	1.0682E-04
2^{-7}	1.8115E-01	7.2172E-02	2.2604E-02	6.6904E-03	2.0359E-03	6.1478E-04
2^{-9}	1.7937E-01	7.1109E-02	2.2157E-02	6.4944E-03	1.9442E-03	5.6545E-04
E_N	1.8387E-01	7.3646E-02	2.3232E-02	6.9711E-03	2.0359E-03	6.1478E-04
R_N	1.4290	1.7593	1.6596	1.6839	1.7234	1.7508
E_N [7]	8.0732E-03	4.0199E-03	1.6136E-03	4.9272E-04	1.3083E-04	3.3230E-05
R_N [7]	1.0060	1.3169	1.7114	1.9131	1.9771	

Table 12: Example 5.4 with $\delta = 0.5\epsilon$, $\eta = 0.5\epsilon$.

$\epsilon \downarrow N \rightarrow$	2^5	2^6	2^7	2^8	2^9	2^{10}
Maximum absolute errors using FMFEM						
2^{-1}	2.5318E-04	6.3214E-05	1.5801E-05	3.9500E-06	9.8748E-07	2.4687E-07
2^{-3}	2.4397E-03	6.0290E-04	1.5029E-04	3.7546E-05	9.3855E-06	2.3463E-06
2^{-5}	3.6145E-02	7.7019E-03	1.8908E-03	4.6934E-04	1.1727E-04	2.9301E-05
2^{-7}	3.3363E-01	1.3057E-01	3.3566E-02	7.2328E-03	1.7558E-03	4.3895E-04
2^{-9}	3.4741E-01	1.6329E-01	6.0267E-02	1.7701E-02	5.3215E-03	1.6464E-03
E_N	3.4741E-01	1.6329E-01	6.0267E-02	1.7701E-02	5.3215E-03	1.6464E-03
R_N	1.0892	1.4360	1.7675	1.7340	1.6925	1.6847
E_N [7]	1.3101E-01	1.3727E-01	1.2122E-01	6.7667E-02	2.1221E-02	5.4258E-03
R_N [7]	-0.0673	0.1794	0.8411	1.6730	1.9676	

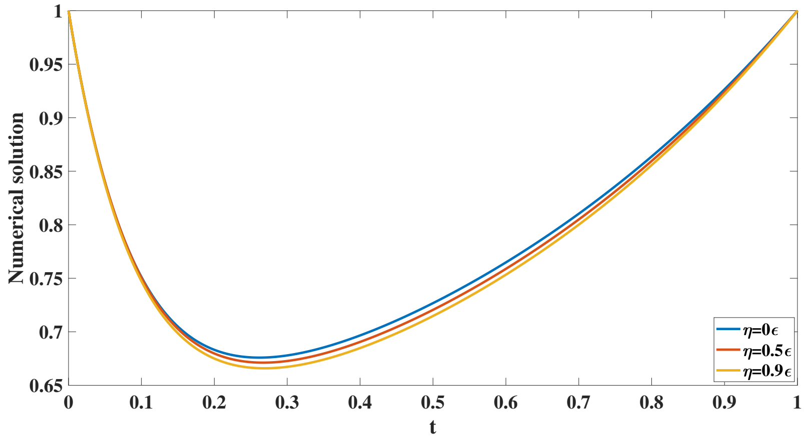

Figure 1: Numerical solution for Example 5.1 with $\epsilon = 0.1$ and $\delta = 0.5\epsilon$ using FMFEM.

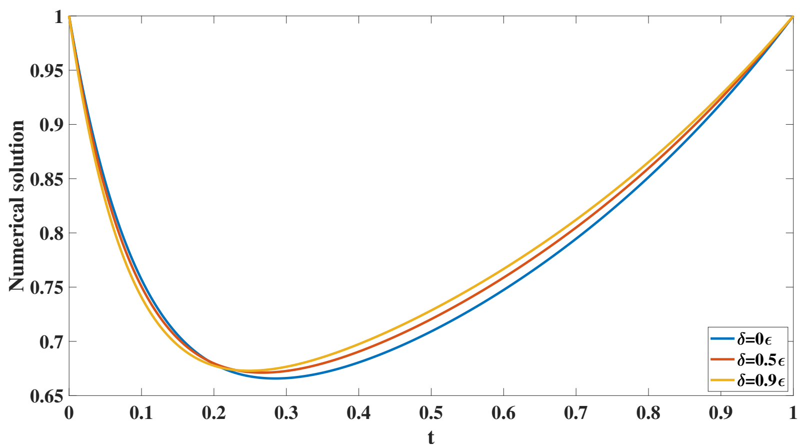

Figure 2: Numerical solution for Example 5.1 with $\epsilon = 0.1$ and $\eta = 0.5\epsilon$ using FMFEM.

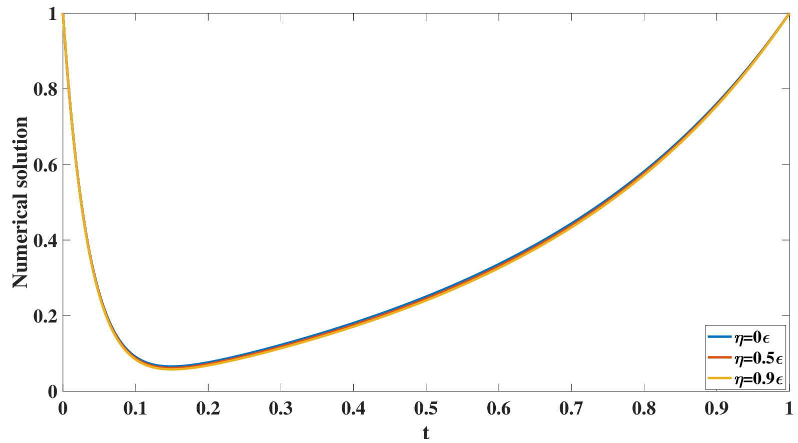

Figure 3: Numerical solution for Example 5.2 with $\epsilon = 0.1$ and $\delta = 0.5\epsilon$ using FOFEM.

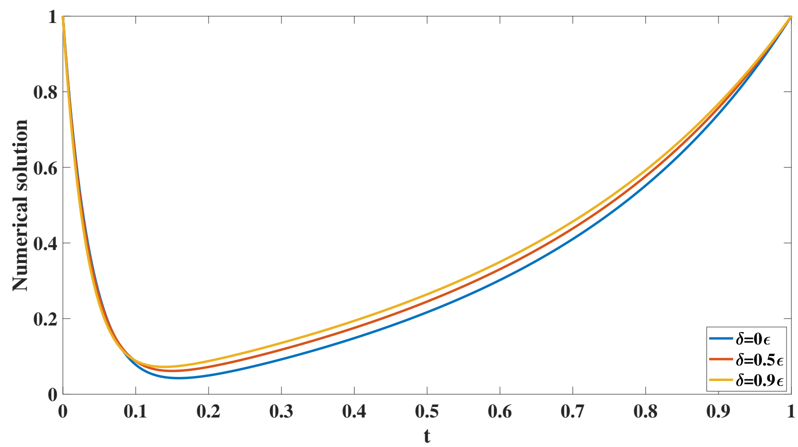

Figure 4: Numerical solution for Example 5.2 with $\epsilon = 0.1$ and $\eta = 0.5\epsilon$ using FOFEM.

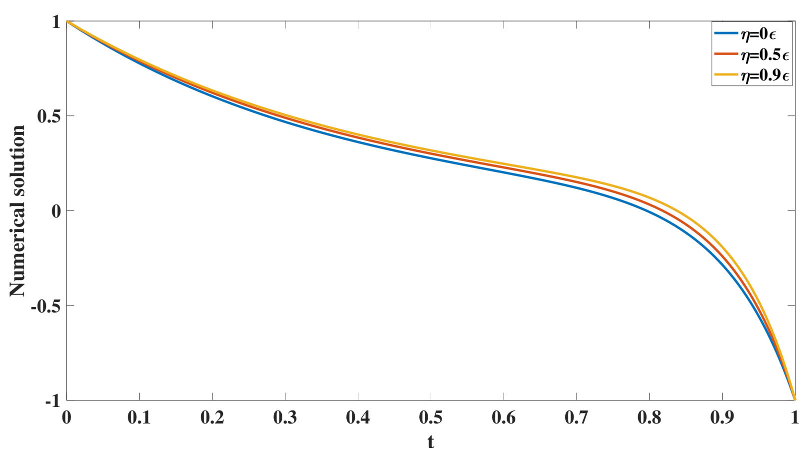

Figure 5: Numerical solution for Example 5.3 with $\epsilon = 0.1$ and $\delta = 0.5\epsilon$ using FMFEM.

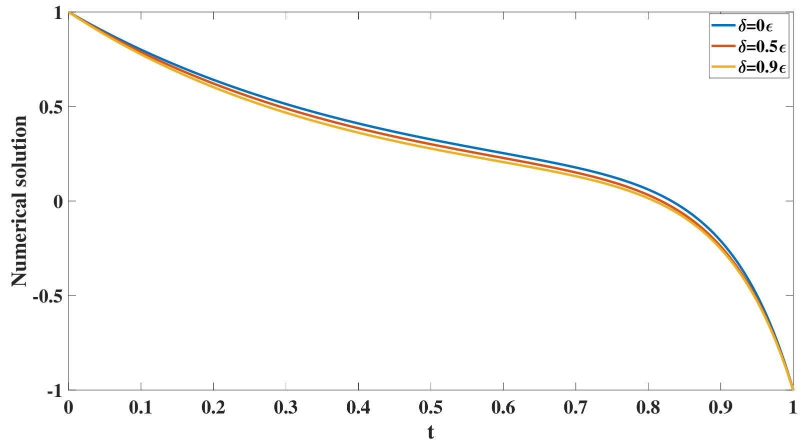

Figure 6: Numerical solution for Example 5.3 with $\epsilon = 0.1$ and $\eta = 0.5\epsilon$ using FMFEM.

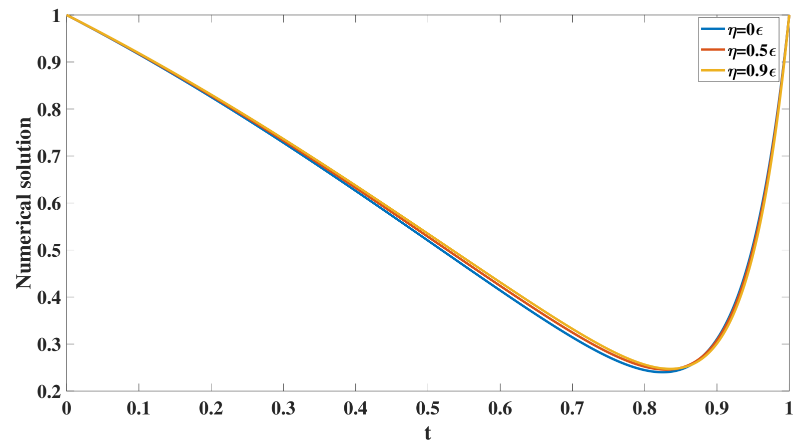

Figure 7: Numerical solution for Example 5.4 with $\epsilon = 0.1$ and $\delta = 0.5\epsilon$ using FOFEM.

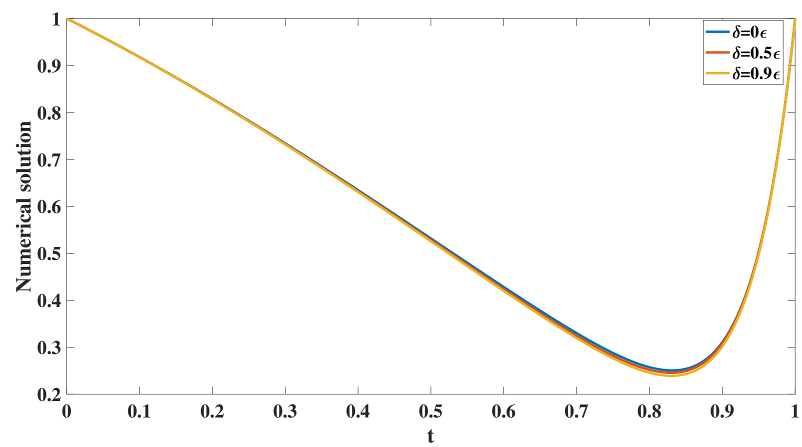

Figure 8: Numerical solution for Example 5.4 with $\epsilon = 0.1$ and $\eta = 0.5\epsilon$ using FOFEM.

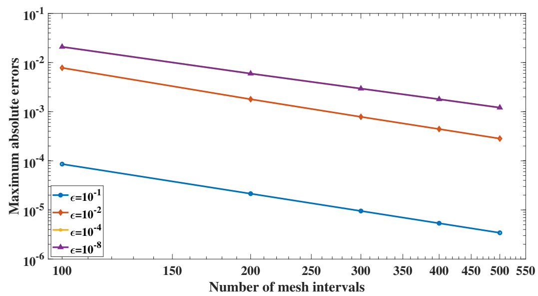

(a) FMFEM

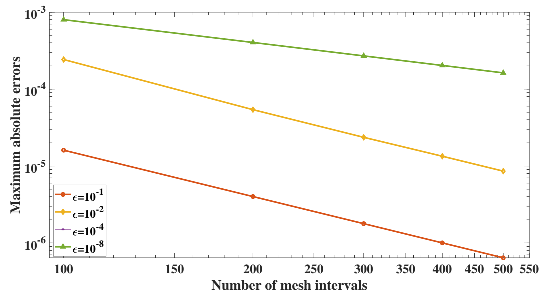

(b) FOFEM

Figure 9: Log-log plot of maximum absolute errors for Example 5.1.

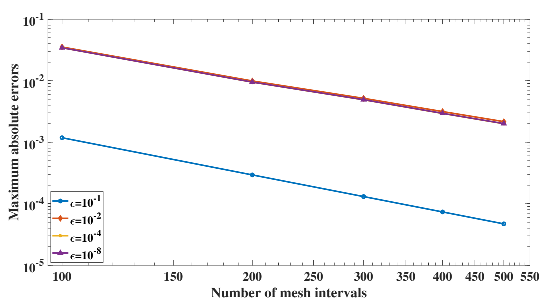

(a) Example 5.2 using FMFEM

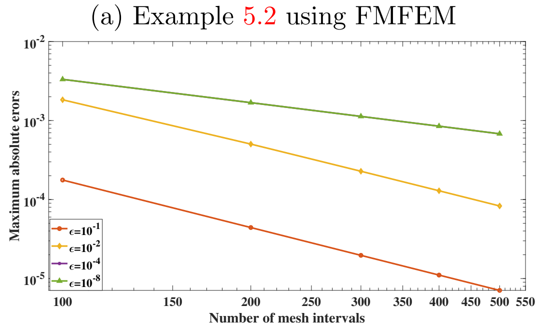

(b) Example 5.2 using FOFEM

Figure 10: Log-log plot of the maximum absolute errors for Example 5.2.

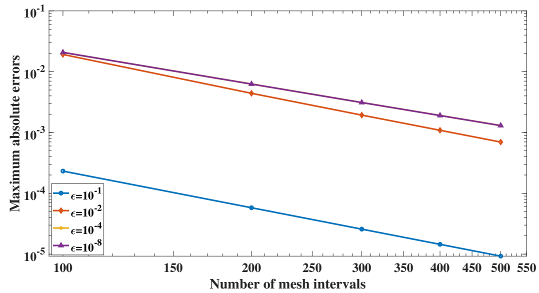

(a) Example 5.3 using FMFEM

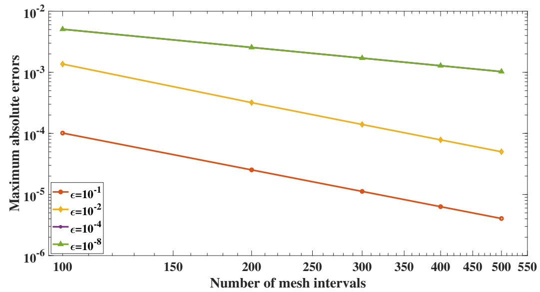

(b) Example 5.3 using FOFEM

Figure 11: Log-log plot of the maximum absolute errors for Example 5.3.

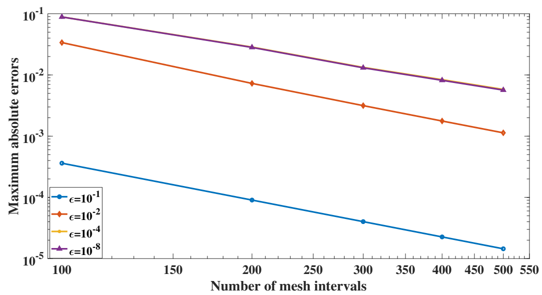

(a) Example 5.4 using FMFEM

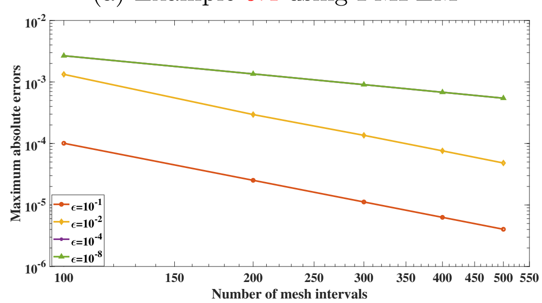

(b) Example 5.4 using FOFEM

Figure 12: Log-log plot of the maximum absolute errors for Example 5.4.

Declarations

Funding

Not Applicable

Ethical Approval

Not Applicable

Availability of supporting data

Not Applicable.

Conflict of interest/Competing interests

The authors declare that they have no conflict of interest, relevant to the content of this article.

Authors' contributions

Both the authors contributed equally to this work.

Acknowledgments

We would like to express our sincere gratitude to the referees for their suggestions to enhance the quality of this work.

References

1. Morton, K. W., *Numerical Solution of Convection-Diffusion Problems*, Appl. Math. Math. Comput. 12, Chapman & Hall, London, (1996).
2. Roos, H.-G., Stynes, M., Tobiska, L., *Robust Numerical Methods for Singularly Perturbed Differential Equations*, 2nd ed., Springer Ser. Comput. Math. 24, Springer, Berlin, (2008).
3. Rihan, F. A., *Delay Differential Equations and Applications to Biology*, Springer Nature, Singapore, (2021).
4. Nayfeh, A. H., Chin, C., Pratt, J., *Perturbation methods in nonlinear dynamics—applications to machining dynamics*, J. Manuf. Sci. Eng. 119(4A), 485–493, (1997).
5. Prathap, T., Rao, R. N., *Fitted mesh methods based on non-polynomial splines for singularly perturbed boundary value problems with mixed shifts*, AIMS Math. 9(10), 26403–26434, (2024).
6. Ravi Kanth, A. S. V., Kumar, P. M. M., *A numerical approach for solving singularly perturbed convection delay problems via exponentially fitted spline method*, Calcolo 54(3), 943–961, (2017).
7. Ranjan, R., Prasad, H. S., *A novel approach for the numerical approximation to the solution of singularly perturbed differential-difference equations with small shifts*, J. Appl. Math. Comput. 65, 403–427, (2021).
8. Vivek, K., Rao, R. N., *Fitted operator methods for singularly perturbed differential-difference equations via splines*, Comput. Math. Math. Phys. 65, 252–269, (2025).
9. Kadalbajoo, M. K., Sharma, K. K., *Numerical treatment of a mathematical model arising from a model of neuronal variability*, J. Math. Anal. Appl. 307(2), 606–627, (2005).
10. Kadalbajoo, M. K., Patidar, K. C., Sharma, K. K., *ϵ-Uniformly convergent fitted methods for the numerical solution of the problems arising from singularly perturbed general DDEs*, Appl. Math. Comput. 182(1), 119–139, (2006).
11. Sirisha, L., Phaneendra, K., Reddy, Y. N., *Mixed finite difference method for singularly perturbed differential-difference equations with mixed shifts via domain decomposition*, Ain Shams Eng. J. 9(4), 647–654, (2018).
12. Conor, J. F., *A class of finite-element methods for singularly perturbed second-order differential equations*, J. Comput. Appl. Math. 34(3), 269–280, (1991).
13. Singh, S., Kumar, D., Deswal, K., *Trigonometric B-spline based ϵ-uniform scheme for singularly perturbed problems with Robin boundary conditions*, J. Differ. Equ. Appl. 28, 924–945, (2022).
14. Singh, S., Kumar, D., *Spline-based parameter-uniform scheme for fourth-order singularly perturbed differential equations*, J. Math. Chem. 60, 1872–1902, (2022).
15. Singh, S., Kumar, D., Shanthi, V., *Uniformly convergent scheme for fourth-order singularly perturbed convection-diffusion ODE*, Appl. Numer. Math. 186, 334–357, (2023).
16. Ayalew, M., Kiltu, G. G., Duressa, G. F., *Fitted numerical scheme for second-order singularly perturbed differential-difference equations with mixed shifts*, Abstr. Appl. Anal., (2021).
17. Kumar, D., *Fitted mesh method for a class of singularly perturbed differential-difference equations*, Numer. Math. Theor. Meth. Appl. 8(4), 496–514, (2015).
18. Farshid, M., Seyede, F. H., *Solving singularly perturbed differential-difference equations arising in science and engineering with Fibonacci polynomials*, Results Phys. 3, 134–141, (2013).

19. Priyadarshana, S., Sahu, S. R., Mohapatra, J., *Asymptotic and numerical methods for solving singularly perturbed differential-difference equations with mixed shifts*, Iran. J. Numer. Anal. Optim. 12(1), 55–72, (2022).

20. Kadalbajoo, M. K., Arjun, S. Y., Kumar, D., *Comparative study of singularly perturbed two-point BVPs via: Fitted-mesh finite difference method, B-spline collocation method and finite element method*, Appl. Math. Comput. 202(2), 713–725, (2008).

21. Mushahary, P., Sahu, S. R., Mohapatra, J., *A parameter uniform numerical scheme for singularly perturbed differential-difference equations with mixed shifts*, J. Appl. Comput. Mech. 6(2), 344–356, (2020).

22. Rai, P., Sharma, K. K., *Numerical study of singularly perturbed differential-difference equation arising in the modeling of neuronal variability*, Comput. Math. Appl. 63, 118–132, (2012).

23. Senthilkumar, L. S., Subburayan, V., Agarwal, R. P., *Asymptotic streamline diffusion finite element method for singularly perturbed convection-diffusion differential-difference equations*, Math. Methods Appl. Sci. 46(10), 11509–11522, (2023).

24. Liu, S. T., Xu, Y., *Galerkin methods based on Hermite splines for singular perturbation problems*, SIAM J. Numer. Anal. 43(6), 2607–2623, (2006).

25. Constantinou, P., Xenophontos, C., *Finite element analysis of an exponentially graded mesh for singularly perturbed problems*, Comput. Methods Appl. Math. 15(2), 135–143, (2015).

26. Swamy, D. K., Phaneendra, K., Reddy, Y. N., *Solution of singularly perturbed differential-difference equations with mixed shifts using Galerkin method with exponential fitting*, Chin. J. Math., (2016).

27. Varga, R. S., *Matrix iterative analysis*, Prentice-Hall Inc., Englewood Cliffs, New Jersey, (1962).

28. Young, D. M., *Iterative solution of large linear systems*, Academic Press, New York, (1971).

Vivek K.,
Department of Mathematics, School of Advanced Sciences,
Vellore Institute of Technology, Vellore,
Tamil Nadu, India.
E-mail: viveksiva154@gmail.com

and

R. Nageshwar Rao,
Department of Mathematics, School of Advanced Sciences and
Department of Database Systems, School of Computer Science and Engineering,
Vellore Institute of Technology, Vellore,
Tamil Nadu, India.
Email: nag.ragi@gmail.com